EVS27
Barcelona, Spain, November 17-20, 2013

DWT-based SOH prediction using the output voltage deviation among the cells in the $LiFePO_4$ battery pack for ESS applications

Jonghoon Kim*, Jongseop Kwak, T. Ishikawa
Energy Storage System (ESS) Development Team, Energy Solution (ES) Business Division, Samsung SDI, Sungsung-dong, Seobuk-gu, Cheonan, Chungcheongnam-do, qwzxas@hanmail.net

Abstract

Electrochemical differences, namely voltage variance among the cells in the $LiFePO_4$ battery pack (rack) is generally related to degradation period, then the magnitude of the voltage variance of the degraded battery pack is increased when compared to the other case of non-degraded battery pack. Therefore, this approach gives insight to the design and implementation of the improved state-of-health (SOH) prediction based on the discrete wavelet transform (DWT) suitable for analysing and evaluating output voltage signal deviation (OVSD) among the cells in the $LiFePO_4$ battery pack for energy storage system (ESS) applications. The discharging/charging voltage signal (DCVS) is applied as source data in the DWT-based analysis due to its ability to extract information from the non-stationary and transient phenomena simultaneously in both the time and frequency domain. By using the wavelet decomposition including the multi-resolution analysis (MRA), the SOH information among the cells in the $LiFePO_4$ battery pack can be extracted from signals including approximation A_n and detail D_n components over a wide frequency range. In addition, through the statistical analysis of the DCVS and two components among the cells for comparison between degraded and non-degraded battery packs, appropriate SOH of an arbitrary pack can be predicted. Verification results indicate the robustness of the proposed approach for the reliable SOH.

Keywords: Discrete wavelet transform (DWT), State-of-health (SOH), Energy storage system (ESS), $LiFePO_4$

1 Introduction

With the process of the storing technology, many applications of the energy storage system (ESS) to the power systems become feasible (Fig. 1) [1]. The ESS consists of multiple cells in series and parallel to meet the energy and voltage requirements for high-power applications. In general, after degradation with use, it has been observed that individual cells in a real battery pack typically show some variation in performance

Figure1: Energy storage system (ESS) of Samsung SDI

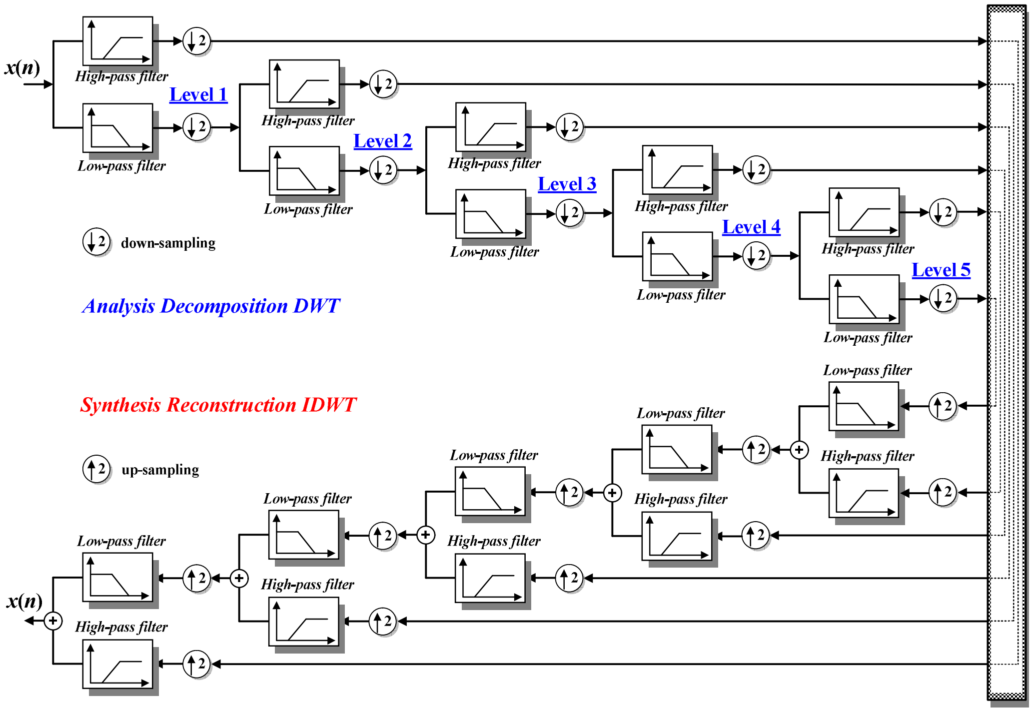

Figure2: DWT-based decomposition and reconstruction processes

depending on the specific operating conditions. With continuous cycling, the variance among the cells is more increased. Therefore, in order to check the current life status and to guarantee the overall system performance, an accurate and reliable knowledge of the state-of-health (SOH) absolutely need to be taken into account in battery management system (BMS).
This approach deals with discrete wavelet transform (DWT)-based approach for SOH prediction of the $LiFePO_4$ battery pack (rack). The DWT is becoming powerful in the analysis of the output voltage signal (OVS) with a non-stationary and transients phenomena [2]. One of its feature is multi-resolution analysis (MRA) with a vigorous function of both time and frequency localization. Through DWT-based MRA requiring filtering and down-sampling, the SOH information among the cells in the $LiFePO_4$ battery pack can be extracted. The DWT decomposes the OVS into time and frequency domains and focuses on short time intervals for high frequency component (detail D_n) and on long time intervals for low frequency component (approximation A_n). From statistical analysis such as standard deviation of the A_n and D_n component among the cells for comparison between degraded and non-degraded battery packs it is possible to predict an appropriate SOH of an arbitrary battery pack. Experimental results show the DWT-based approach is clearly appropriate for the reliable SOH prediction. This approach has been validated by extensive experimental results conducted on 10 prismatic $LiFePO_4$ battery pack comprised of 70 cells in series connection (70S1P) that had a rated capacity of 50Ah produced by Samsung SDI.

2 Discrete wavelet transform (DWT)

The DWT has The DWT has been widely used for a new mathematical approach that decomposes a time domain signal into different frequency groups, and provides an effective manner for analyzing the non-stationary signals, rather than conventional Fourier transform which can only give the information in the frequency domain [3][4]. The DWT defines as the inner product of a signal $x(t)$ with the mother wavelet $\psi(t)$ in (1).

$$DWT(a,b) = \frac{1}{\sqrt{2^j}} \int_{-\infty}^{\infty} x(t)\psi^*\left(\frac{t-k2^j}{2^j}\right)dt \qquad (1)$$

This defines a dyadic orthonormal wavelet transform and provides the basis for MRA. In MRA process, any time series $x(t)$ can be completely decomposed in terms of approximations, provided by scaling function $\phi_{j,k}(t)$ and the details, provided by the wavelet function $\psi_{j,k}(t)$, and are defined as (2) and (3), respectively.

$$\phi_{j,k}(t) = 2^{-\frac{j}{2}}\phi(2^{-j}t-k) \qquad (2)$$

$$\psi_{j,k}(t) = 2^{-\frac{j}{2}}\psi(2^{-j}t-k) \qquad (3)$$

As expressed in (4) and (5), the scaling function is associated with the low-pass filter $h(n)$, and the

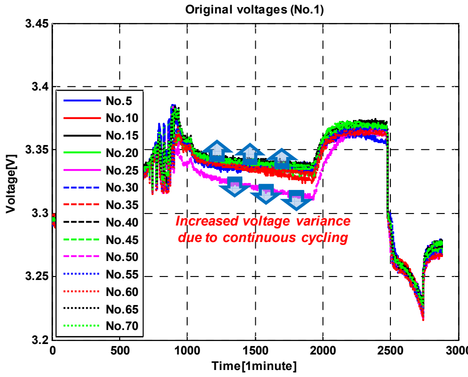

Figure3: Increased voltage variance due to continuous cycling among the $LiFePO_4$ cells (original signal)

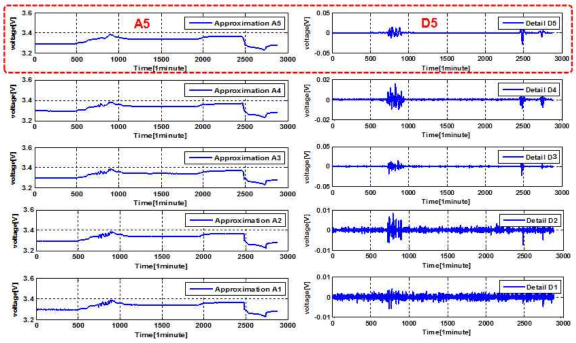

Figure4 : Approximation A_n and detail D_n components based on the DWT

wavelet function is associated with the high-pass filter $g(n)$.

$$\phi(t) = \sqrt{2}\sum_n h(n)\phi(2t-n) \tag{4}$$

$$\psi(t) = \sqrt{2}\sum_n g(n)\phi(2t-n) \tag{5}$$

As shown in Fig. 2, the DWT algorithm uses low /high pass filters in the wavelet decomposition and reconstruction processes. The MRA leads to a hierarchical and fast scheme, and it can be implemented by a set of successive filter banks. Considering the filter bank implementation in Fig. 2, the relationship of the approximation coeff-icients $a_{j,k}$ and detail coefficients $d_{j,k}$ between adjacent levels at level j are given as (6) and (7).

$$a_{j,k} = \sum_n h(n-2k)a_{j-1,n} \tag{6}$$

$$d_{j,k} = \sum_n g(n-2k)a_{j-1,n} \tag{7}$$

Because $x(t)$ has a length of 2^N, there is a maximum of N levels, or a maximum $N(J\leq N)$ of applications of $h(n)$ and $g(n)$. Therefore, the J-level DWT representation of a signal $x(t)$ can be defined as (8).

$$x(t) = \sum_{k=0}^{2^{N-j}-1} a_{j,k}2^{-\frac{j}{2}}\phi(2^{-j}t-k) + \sum_{j=1}^{J}\sum_{k=0}^{2^{N-j}-1} d_{j,k}2^{-\frac{j}{2}}\psi(2^{-j}t-k) \tag{8}$$

Each set of wavelet transform coefficients $a_{j,k}$ and $d_{j,k}$ for $1\leq j\leq J$, represents a band-pass filtered

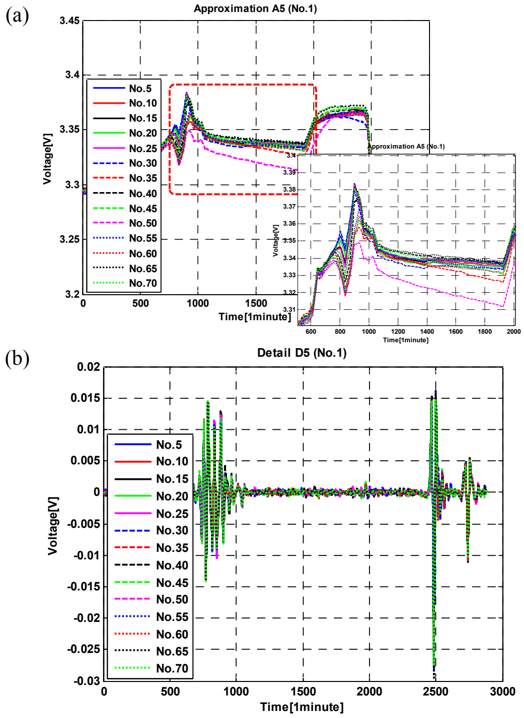

Figure5: Two components of the $LiFePO_4$ battery pack (No.1), (a) Approximation A_5, (b) detail D_5

and down-sampled version of the original signal $x(t)$. The low-pass analysis filter and the high-pass analysis filter are combined with down-sampling operations. The decomposition process can be iterated, with successive approximations being decomposed in turn, so that a signal $x(t)$ is broken down into many lower resolution components, called as the wavelet decomposition tree. In the filtering process, for a generic detail D_n, the upper limit of its frequency band coincides with the lower limit of the band of the previous detail D_{n-1}, and its bandwidth is half the bandwidth of the previous detail. Therefore, a detail D_n contains the information concerning the signal components with frequencies included within the interval $[2^{-(n+1)}f_s, 2^{-n}f_s]$Hz. On the other hand, the appro-ximation A_n contains the low frequency com-ponents of the original signal $x(t)$ included in the interval $[0, 2^{-(n+1)}f_s]$Hz. Similarly, the synthesis filter bank consists of the low-pass synthesis filter and the high-pass synthesis filter with up-sampling operation.

3 Proposed approach

3.1 Decomposition of the DCVS as a terminal voltage

The ESS in this proposed approach is used as energy storage for grid connected photovoltaic (PV) power system. This power system was

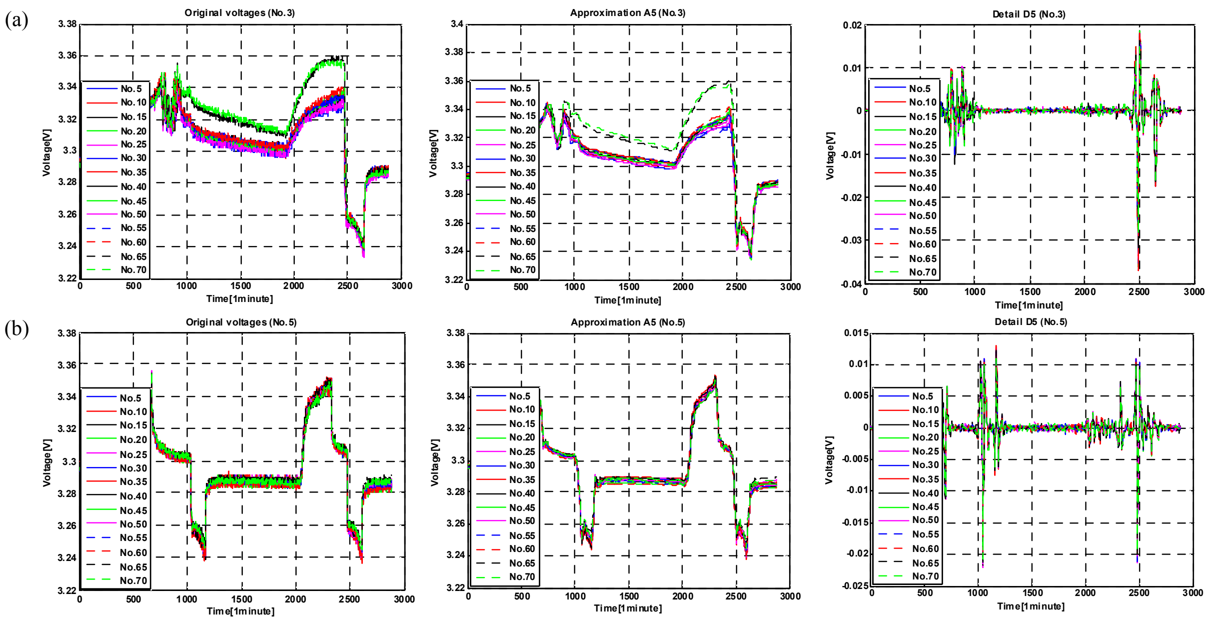

Figure6 : DCVSs and two components (approximation A_5 and detail D_5) of the two $LiFePO_4$ battery packs (a) No.3, (b) No.5

designed to have adequate generation from grid connected PV and ESS. According to daily demand for customer, the system provides the energy to load through maintaining the balance between the amount of discharging/charging stored energy and PV. Therefore, all discharging/ charging currents of the ESS applied to the 10 prismatic $LiFePO_4$ battery pack are different.

As aforementioned, due to degradation with use, it has been apparent that individual cells in a battery pack show some variation in performance, and the variance among the cells is gradually increased (Fig. 3 of No.1 battery pack). For reference, due to the limitation of simultaneous drawing of 70 cells, 14 cells were selected in the entire cell's number range at each 5 cell's number interval. For a discharging/charging current of an ESS, the DCVS is obtained. For analysis and evaluation of the DCVS with a non-stationary and transients, five-level decomposition of the MRA is implemented for extracting information from these phenomena. The orthogonal wavelet filter 'dB3' of the Daubechies family that suitable for a wide of application is selected as the optimum wavelet function of the proposed work. According to five-level decomposition process implementing the down-sampling ⇩2 of the MRA, approximation (A_1~A_5) and detail (D_1~D_5) components are measured, as illustrated in Fig. 4. Then, A_5 with the lowest frequency band and D_5 among high frequency D_1~D_5 are selected as the decision components for provision of SOH information. Two components including A_5 and D_5 among 14 cells of the pack (No.1) are

Table1: Standard deviation among 14 cells (DCVS)

Cell	Standard D.	Cell	Standard D.	Cell	Standard D.
No.5	0.035099	No.10	0.034938	No.15	0.034994
20	0.034610	25	0.034659	30	0.034021
35	0.033722	40	0.035657	45	0.035878
50	0.032827	55	0.035987	60	0.035743
65	0.036270	70	0.036108		***0.001005***

Table2: Standard deviation among 14 cells (approximation A_5)

Cell	Standard D.	Cell	Standard D.	Cell	Standard D.
No.5	0.034929	No.10	0.034770	No.15	0.034834
20	0.034443	25	0.034483	30	0.033868
35	0.033586	40	0.035509	45	0.035730
50	0.032684	55	0.035844	60	0.035601
65	0.036102	70	0.035945		***0.001003***

Table3: Standard deviation among 14 cells (detail D_5)

Cell	Standard D.	Cell	Standard D.	Cell	Standard D.
No.5	0.002436	No.10	0.002455	No.15	0.002420
20	0.002408	25	0.002464	30	0.002226
35	0.002054	40	0.002262	45	0.002199
50	0.002022	55	0.002222	60	0.002194
65	0.002502	70	0.002441		***1.5878×10^{-4}***

Table4: Standard deviation of the DCVS and two components of the 10 $LiFePO_4$ battery packs

Rack	Standard D.(ori)	Standard D.(A_5)	Standard D.(A_5)
No.1	0.001005	0.001003	1.5878×10^{-4}
2	3.8307×10^{-4}	3.9557×10^{-4}	3.8020×10^{-5}
3	0.002286	0.002315	2.3707×10^{-4}
4	0.003574	0.003615	3.5532×10^{-4}
5	6.0594×10^{-4}	6.0160×10^{-4}	6.2436×10^{-5}
6	0.002043	0.002058	2.5878×10^{-4}
7	2.0267×10^{-4}	2.0345×10^{-4}	2.1797×10^{-5}
8	8.1114×10^{-4}	8.2169×10^{-4}	8.7638×10^{-5}
9	7.0415×10^{-4}	6.9349×10^{-4}	7.1338×10^{-5}
10	5.0106×10^{-4}	4.9937×10^{-4}	4.9039×10^{-5}

shown in Fig. 5. Statistical analysis of standard deviation of the DCVS and two components (A_5

Table5: Proposed SOH prediction based on the DWT for ESS (DCVS, approximation component, and detail component)

$SOH_{ori}^{predict} = 1 - \frac{\lvert A_{ori} - B_{ori} \rvert}{0.5 \times \alpha A_{ori}}$	$0 \le SOH_{ori}^{predict} \le 1$	$SOH_{ori}^{predict} = 0 \;\; if \;\; B_{ori} = (1 + 0.5\alpha) A_{ori}$	$SOH_{ori}^{predict} = 1 \;\; if \;\; B_{ori} = A_{ori}$
$SOH_{app}^{predict} = 1 - \frac{\lvert A_{app} - B_{app} \rvert}{0.5 \times \beta A_{app}}$	$0 \le SOH_{app}^{predict} \le 1$	$SOH_{app}^{predict} = 0 \;\; if \;\; B_{app} = (1 + 0.5\beta) A_{app}$	$SOH_{app}^{predict} = 1 \;\; if \;\; B_{app} = A_{app}$
$SOH_{det}^{predict} = 1 - \frac{\lvert A_{det} - B_{det} \rvert}{0.5 \times \tau A_{det}}$	$0 \le SOH_{det}^{predict} \le 1$	$SOH_{det}^{predict} = 0 \;\; if \;\; B_{det} = (1 + 0.5\tau) A_{det}$	$SOH_{det}^{predict} = 1 \;\; if \;\; B_{det} = A_{det}$

- Standard deviation among cells for non-degraded (fresh) : A_{ori}(1.50321×10^{-4}; DCVS), A_{app}(approximation; 1.53147×10^{-4};), A_{det} (detail; 1.68235×10^{-4})
- Standard deviation among cells for degraded pack (aged) : B_{ori} (DCVS), B_{app} (approximation), B_{det} (detail)
- α, β, τ : the ratio between maximum/maximum values of the standard deviations of 10 packs (DCVS:17.63, approximation:17.76, detail:16.30)

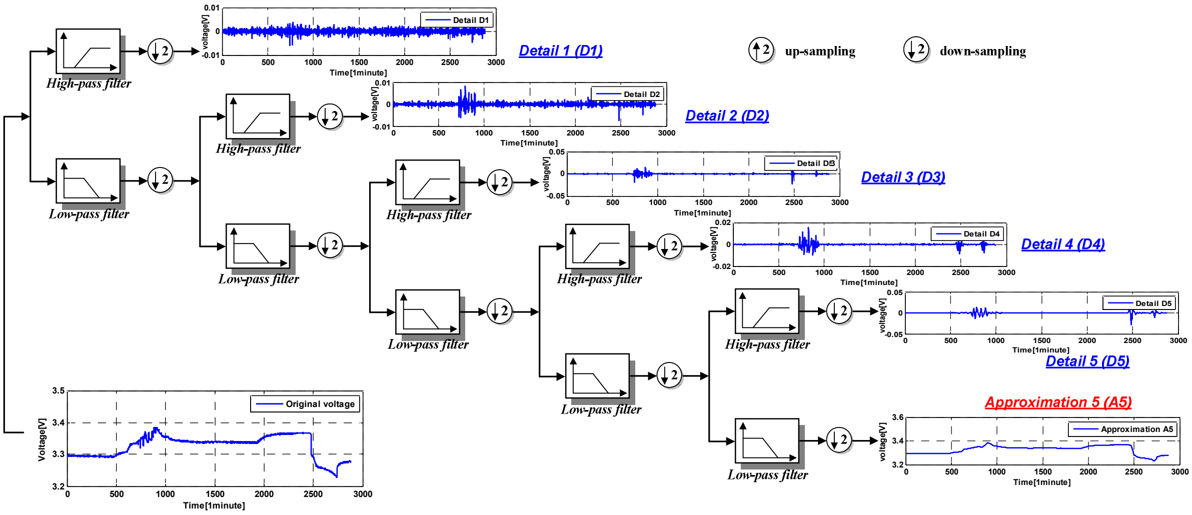

Figure7: Decomposition process of the DWT-based proposed approach.

$$SOH_{total}^{predict} = \frac{SOH_{ori}^{predict} + SOH_{app}^{predict} + SOH_{det}^{predict}}{3} \qquad 0 \le SOH_{total}^{predict} \le 1 \qquad (9)$$

and D_5) are can be respectively done, as listed in Table 1 through 3. First of all, each standard deviation of 14 cells is measured (first step). Final standard deviation among 14 cells that have each standard deviation value previously measured at the first step. As listed in these tables, two cells of 35 and 50 of the battery pack (No.1) have smallest standard deviations. It can be shown that voltage variance is clearly related to degradation period, then the magnitude of the voltage variance of the degraded cell is increased when compared to the other case of non-degraded cell. DWT-based decomposition is identically applied to the other $LiFePO_4$ battery packs of Nos.2~10 (Table 4 and Fig. 6 : Nos.3 and 5).

3.2 SOH prediction

In this work, DWT-based SOH prediction for ESS is newly introduced (Table V). As expressed in (9), the SOH of an arbitrary pack can be expressed as the sum of three values including $SOH_{ori}^{predict}, SOH_{app}^{predict}, SOH_{det}^{predict}$. For example, the predicted SOH value of No. 4 pack is calculated as (10).

$$SOH_{ori}^{predict} = 1 - \frac{\lvert A_{ori} - B_{ori} \rvert}{0.5 \times \alpha A_{ori}} = 1 - \frac{\lvert 1.50321 \times 10^{-4} - 0.003574 \rvert}{0.5 \times 17.63 \times 1.50321 \times 10^{-4}} = 0.3540$$

$$SOH_{app}^{predict} = 1 - \frac{\lvert A_{app} - B_{app} \rvert}{0.5 \times \beta A_{app}} = 1 - \frac{\lvert 1.53147 \times 10^{-4} - 0.003615 \rvert}{0.5 \times 17.76 \times 1.53147 \times 10^{-4}} = 0.3715$$

$$SOH_{det}^{predict} = 1 - \frac{\lvert A_{det} - B_{det} \rvert}{0.5 \times \tau A_{det}} = 1 - \frac{\lvert 1.68235 \times 10^{-5} - 3.55320 \times 10^{-4} \rvert}{0.5 \times 16.30 \times 1.68235 \times 10^{-4}} = 0.3828$$

$$SOH_{total}^{predict} = \frac{SOH_{ori}^{predict} + SOH_{app}^{predict} + SOH_{det}^{predict}}{3} = \frac{0.3540 + 0.3715 + 0.3828}{3} = 0.3694 \qquad (10)$$

4 Conclusion

This approach gives insight to the design and implementation of the improved SOH prediction based on the DWT suitable for analyzing and evaluating output voltage signal deviation among the cells in the $LiFePO_4$ battery pack for ESS applications.

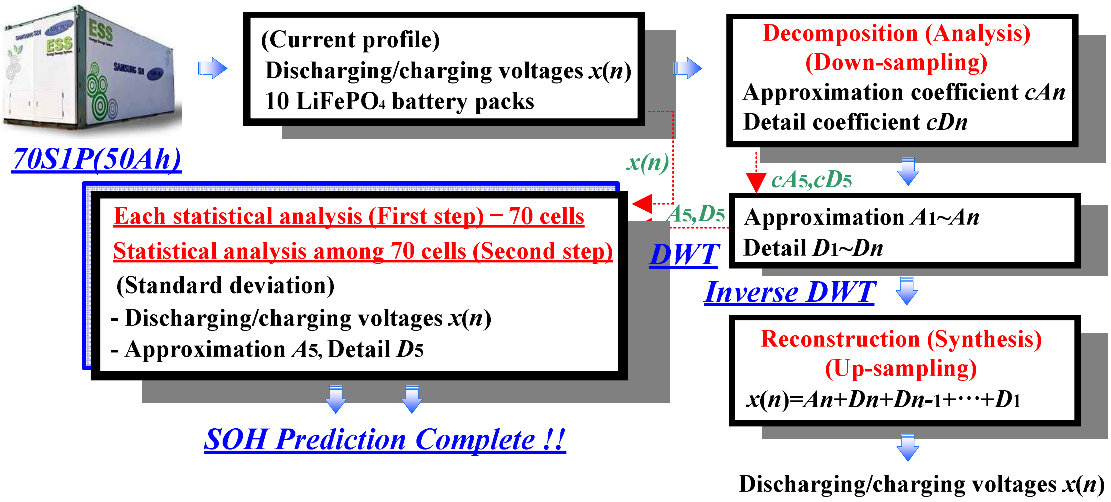

Figure8: Schematic diagram of the proposed approach

Acknowledgments

This research was conducted under Samsung SDI, Co. Ltd., Republic of Korea.

References

[1] H. Qian, J. Zhang, J.-S. Lai, and W. Yu, "A High-Efficiency Grid-Tie Battery Energy Storage System," *IEEE Trans. Power Electron.*, Vol. 26, No. 3, pp. 886-895, Mar. 2011.

[2] A. Y. Goharrizi and N. Sepehri, "A Wavelet-Based Approach to Internal Seal Damage Diagnosis in Hydraulic Actuators," *IEEE Trans. Ind. Electron.*, vol. 57, no. 5, pp. 1755–1763, May. 2010.

[3] M. R.-Guasp, J. A. A.-Daviu, M, P.-Sanchen, R. P.-Panadero, and J. P.-Cruz, "A General Approach for the Transient Detection of Slip-Dependent Fault Components Based on the Discrete Wavelet Transform," *IEEE Trans. Ind. Electron.*, vol. 55, no. 12, pp. 4167–4180, Dec. 2008.

[4] D. Giaouris, J. W. Finch, O. C. Ferreira, R. M. Kennel, and G. M,. El-Murr, "Wavelet Denoising for Electric Drives," *IEEE Trans. Ind. Electron.*, vol. 55, no. 2, pp. 543–550, Feb. 2008.

Authors

Jonghoon Kim received the Ph.D degrees in electrical engineering and computer science from Seoul National University, Seoul, Republic of Korea, in 2012. Dr. Kim is currently working as a Senior Research Engineer in Energy Storage System (ESS) development team, Energy Solution (ES) Division, Samsung SDI, Cheonan, Republic of Korea. His main research interests include battery management system (BMS; modeling, screening, equalization, SOC/SOH estimation, and firmware design) and fuel cell system (ripple current analysis, SOH prediction, and modeling).